

Modeling a MEMS Thermal Conductivity Pressure Sensor for the Evaluation of Glass Frit Vacuum Packaging

Kerry Cheung

Department of Electrical Engineering and Computer Science
Massachusetts Institute of Technology, Cambridge

Abstract: Developing an accurate model for MEMS devices and structures is a great asset for future design optimization and provides insight into experimental results. A thermal conductivity pressure sensor was microfabricated to evaluate the success of a glass frit vacuum packaging scheme. The sensor and the package dimensions present classical size effects that must be included in the model for accuracy. It was found that the experimental data correlates quite well with the developed model but with a few shortcomings.

Introduction

Portable power has been an important demand in our technologically advanced society. From laptops and cellular phones, to unmanned military probes and battle field electronics, high density compact power is needed. The majority of current portable power sources are lithium-ion batteries but they may soon fall behind on the increasing demand for higher power densities. An attractive option is to take advantage of the high energy to weight ratios associated with combustible fuels.

Fuel cell systems, microengines, thermoelectric, and thermophotovoltaics are several power generation schemes that utilize these fuels. Extensive work has been done on the fuel cell systems and thermophotovoltaics but both require a vacuum environment for efficient energy conversion. Poor thermal isolation degrades device performance substantially so a simple solution is to use a vacuum package to minimize the heat loss.

Methods such as anodic bonding, silicon fusion bonding, and intermediate material bonding with solder or glass frit is known to

be capable of producing a hermetic seal. Intermediate material bonding is the optimal bonding method for the fuel cell and thermophotovoltaic systems due to the constraints imposed by the device design and fabrication processes. Glass frit is the ideal material to use since it is relatively versatile, electrically insulating, and has excellent reflow characteristics.

A thermal conductivity pressure sensor consisting of a platinum heating element sitting on a silicon nitride membrane was fabricated as a test structure. Power dissipated in the resistor has a direct correlation to the pressure within the package and is used as the sensing mechanism [1]. The device is designed to permit a four-point probe measurement to be taken after a successful bond. The purpose of the measurement is to determine whether the desired vacuum package was achieved or not. Developing an accurate model with a thorough understanding of the various heat transport mechanisms involved will be very useful for the interpretation of experimental data.

Materials and Methods

The packaged device consists of a three wafer stack as shown in Figure 1. The top cap has electrical access ports and a shallow cavity to ensure separation between the sensor and package. The device layer contains the sensor and a pressure equilibration hole, while the bottom cap has a deep cavity for the incorporation of getters [1]. The top and bottom caps are fabricated utilizing standard photolithography and DRIE on a SSP wafer. For the top cap, the shallow cavity is etched to 25 μm followed by a target mount, and a backside through etch to form the electrical access ports. For the bottom cap, a 250 μm etch is performed to create the getter cavity. The device layer is a DSP wafer that is initially coated with 100 nm of low stress nitride. The KOH hard mask for the membrane and pressure equilibration hole is defined on the backside using RIE. Lift-off techniques are then used to deposit a 10 nm adhesion layer of Ta, 400 nm of Pt, followed by a 20 nm barrier layer of Ta to form the sensor. The device wafer is then placed in 20% KOH at 85°C for ~5 hours, utilizing a special chuck to protect the metallization, to create the membrane. The wafer is then annealed at 650°C for 1 hour to prevent electrical drifts in the device.

The wafers are die-sawed and cleaned with acetone and DI water. A glass frit tape, GPR-10 from Vitta Corp, is transferred onto the capping wafers. The fritted pieces are placed in a box furnace at 450°C for 10 hours to burn off the organic binder. The pieces are cleaned once again, and then stacked in a custom made copper chuck for bonding in a vacuum system assembled with components from Kurt J. Lesker. The chamber is pumped down to 20 mTorr with a Trivac B D25B mechanical roughing pump before the bonding cycle is initiated.

The heating is accomplished by a temperature controller (CNi-32), a solid state relay (SSR240DC25), both from Omega Engineering, and custom cartridge heaters from Watlow. A 30 minute ramp to 300°C is followed by a 60 minute hold to ensure that the pieces have time to outgas. The chuck is then brought to 475°C in a 15 minute ramp followed by a 30 minute hold to perform the bond. The chuck is allowed to cool to room temperature before the system is vented to atmosphere. A four-point probe resistance measurement is made and the package is evaluated against a calibration curve that is created before the bond.

Calibration curves for each device are created utilizing a custom made four-point probe chuck. A HP-E3612A is used to supply a constant current, while a Keithley multimeter is used to measure the voltage drop across the resistor. After taking an initial measurement of the resistance utilizing a very small current (minimal heating), a target resistance corresponding to 87°C is calculated assuming a TCR of 0.38% for Pt. There are several ways to proceed with the calibration but assuming a constant temperature for the resistor is the simplest and the one used. The device, along with the probe chuck, is placed in the vacuum system. The chamber is pumped down and a leak valve is adjusted to produce a fixed vacuum level. The current is adjusted until the device produces a resistance close to the calculated target value and a data point is taken. This data point corresponds to the power dissipated at a fixed temperature and pressure. Data points corresponding to pressures ranging from 1,000 mTorr to 30 mTorr are collected and the calibration curve is generated.

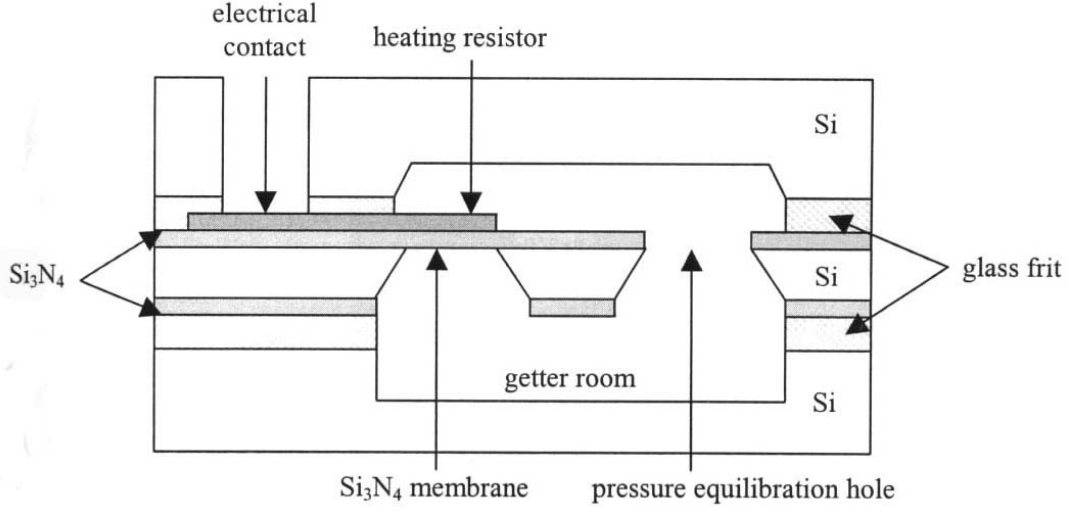


Figure 1 – Device Cross Section [1]

Modeling

To evaluate the performance of the device as a pressure sensor, a model was developed and compared with data obtained in a calibration experiment. The underlying principle used to develop this model is the conservation of energy. Power dissipated in the resistor must equal the flux of heat moving away from the resistor. Heat conduction along the nitride membrane, radiation from the heater, and conduction through gases are the primary heat transport mechanisms. The device is in a sealed packaged so convection through gases is not considered.

Conduction along Membrane

Heat conduction along the membrane was treated using Fourier's Law. Since the silicon nitride is quite thin, we must take classical effects into consideration for an accurate model. Assuming the nitride is an isotropic material and the boundaries are diffusely scattering, we can obtain an equation relating thermal conductivity and size effects. For a free standing thin film, the phonon thermal conductivity with

diffusely scattering boundaries is given by [2],

$$\frac{k}{k_b} = 1 - \frac{3}{8\xi} [1 - 4\langle E_3(\xi) - E_5(\xi) \rangle] \quad (1)$$

$$E_n(x) = \int_0^1 \mu^{n-2} \exp\left(-\frac{x}{\mu}\right) d\mu \quad (2)$$

where k_b is the bulk thermal conductivity of the material, $\xi = d/\Lambda$ is the acoustic thickness, d is the thickness of the film, and Λ is the phonon mean free path in silicon nitride.

To estimate the value of the phonon mean free path, the simple kinetic theory can be used to obtain $k_b = Cv\Lambda/3$, where C is the volumetric specific heat and v is the speed of the carrier in the material [2]. Another option is to utilize the equipartition theorem to derive,

$$\Lambda = \frac{2h\nu}{\kappa_B T} \quad (3)$$

where h is Planck's constant, κ_B is Boltzmann's constant, and T is the temperature of the material [3].

Transport by Radiation

Heat flux from radiation can be modeled rather simply by assuming parallel plate geometry and utilizing the Stefan-Boltzmann Law for radiation. By taking into considering classical size effects and transport through an absorbing, emitting, and scattering medium, a layer of complexity is added to the parallel plate model. Assuming the diffusion approximation is applicable and diffusion-transmission boundary conditions are used, the need to solve for the temperature distribution within the medium is avoided. The heat flux, J_q , between two parallel surfaces is then given by [2],

$$\frac{J_q}{e_{01} - e_{02}} = \frac{1}{\frac{3dK_e}{4} + \frac{1}{\epsilon_1} + \frac{1}{\epsilon_2} - 1} \quad (4)$$

$$K_e = \frac{4\pi\kappa}{\lambda_0} \quad (5)$$

where $e_{0n} = \sigma T_n^4$ is the black body radiation of the n^{th} surface at temperature T_n (σ being the Stefan constant), ϵ_n is the emissivity of the n^{th} surface, d is the spacing between the surfaces, and K_e is the extinction coefficient of the radiation. In equation 5, κ is the material extinction coefficient, and λ_0 is the photon wavelength which can be estimated using Equation 3 (for photons, the 2 in the numerator is replaced by 0.15), or the Wein's Displacement Law $\lambda_0 T = 2167.8 \mu\text{m}\cdot\text{K}$ [2].

Conduction through Gases

Conduction through the gases trapped in the package can also be modeled using the simple Fourier's Law. Since we have low

pressures, thus large mean free paths, and small dimensions, we need to treat the gas as a rarefied gas. Essentially, we have gas trapped between parallel plates, which is similar to the situation for radiation. Utilizing the same assumption as those for the radiation treatment, namely the diffusion approximation and diffusion-transmission boundary conditions, the thermal conductivity is given as [2]

$$\frac{k}{k_b} = \frac{1}{1 + \frac{4\Lambda}{3d}} \quad (6)$$

In the situation of a gas, the mean free path is dependent on pressure. From the kinetic theory of gases, we have

$$\Lambda = \frac{\kappa_B T}{\sqrt{2}\delta^2 P} \quad (7)$$

where δ^2 is the collision cross-sectional area of the gas molecules, and P is the pressure [1].

Combining all three heat transport mechanisms and equating it to the power dissipated in the resistor, we have

$$\begin{aligned} Power = I \cdot V = & \frac{A_{cs-nit} k_{nit} (T - T_0)}{L_{nit}} + \\ & \frac{A_{c-top} k_{air} (T - T_0)}{d_{top}} + \frac{A_{c-bot} k_{air} (T - T_0)}{d_{bot}} + \\ & A_{r-top} J_{r-top} + A_{r-bot} J_{r-bot} \end{aligned} \quad (8)$$

I is the current being passed through the device, V is the voltage measured across the device, T is the effective peak temperature of the device and T_0 is the temperature of the package. A_{cs-nit} is the effective cross section area that heat is transported across the membrane, k_{nit} is the thermal conductivity of

the membrane, and L_{nit} is the effective distance along the membrane that the temperature gradient is established. $A_{c-top/bot}$ is the effective cross sectional area of the air conduction pathway above/below the resistor, k_{air} is the pressure dependent thermal conductivity for air, and $d_{top/bot}$ is the distance from the resistor to the top/bottom of the package. $A_{r-top/bot}$ is the effective surface area that is emitting radiation above/below the resistor, and $J_{r-top/bot}$ is the corresponding heat flux above/below the membrane.

Results

From an extensive literature search, several values for material properties were extracted and are summarized in Table 1 along with assumed dimensions used in the model. Most material properties depend on temperature so the values chosen correspond to those at $T = T_{avg} = 330$ °C, the average temperature seen in the device.

| | |
|-----------------------|--|
| $k_{nit 0}$ | 3.0 W/K-m |
| C_{v-nit} | 1.14×10^6 J/m ³ -K |
| v_{nit-l} | 10.3×10^3 m/s |
| v_{nit-t} | 6.2×10^3 m/s |
| $k_{air 0}$ | 0.0285 W/K-m |
| δ^2 | 4.39×10^{-19} m ² |
| $\epsilon_{nitride}$ | 0.18 |
| $\epsilon_{silicon}$ | 0.65 |
| $\epsilon_{platinum}$ | 0.05 |
| L_{nit} | 100×10^{-6} m |
| d_{nit} | 100×10^{-9} m |
| d_{top} | 25×10^{-6} m |
| d_{bot} | 450×10^{-6} m |
| $A_{r/c-top/bot}$ | $(1.2 \times 1.2) \times 10^{-6}$ m ² |
| A_{cs-nit} | $4(1.2 \times 100) \times 10^{-12}$ m ² |

Utilizing the simple kinetic theory, the mean free path for phonons in the nitride film was calculated to be $\Lambda_{nit} = 1.27$ nm

assuming that the translational mode is the dominant mode for phonons. If Equation 3 was used instead, we would obtain $\Lambda_{nit} = 1.80$ nm which is on the same order of the value obtained from the kinetic theory. In either case, the acoustic thickness ξ is relatively large indicating that the thermal conductivity of the film is close to that of bulk nitride. Assuming that the heat transport along the membrane is isotropically away from the resistor, the heat conduction along the nitride film is calculated to be 0.864 mW.

Since air is the medium in which radiation is passing through, the material extinction coefficient κ is zero. This simplifies the expression in Equation 4 because the extinction coefficient K_e becomes zero as well. The photon wavelength is no longer needed but we can calculate the estimated values for completeness. We obtain 6.55 μ m using the photon version of Equation 3 (replace the 2 with 0.15) while we get 6.57 μ m using the Wein's Displacement Law. These two values are very close and are on the order of d_{top} indicating that classical effects can be potentially important if the gas did not have a zero extinction coefficient. Assuming that the nitride directly beneath the platinum reaches the same temperature as the resistor, the total radiation is calculated to be 0.151 mW.

From Figure 2, we can see that conduction through gases is the dominant heat transport mechanism in the packaged device. A quick calculation shows that the mean free path of air is 55 μ m at $P = 1,000$ mTorr, and is 5.5 mm at $P = 10$ mTorr. Since the mean free paths at the pressures of interest are larger than d_{top} , there is no doubt that the rarefied gas treatment is necessary.

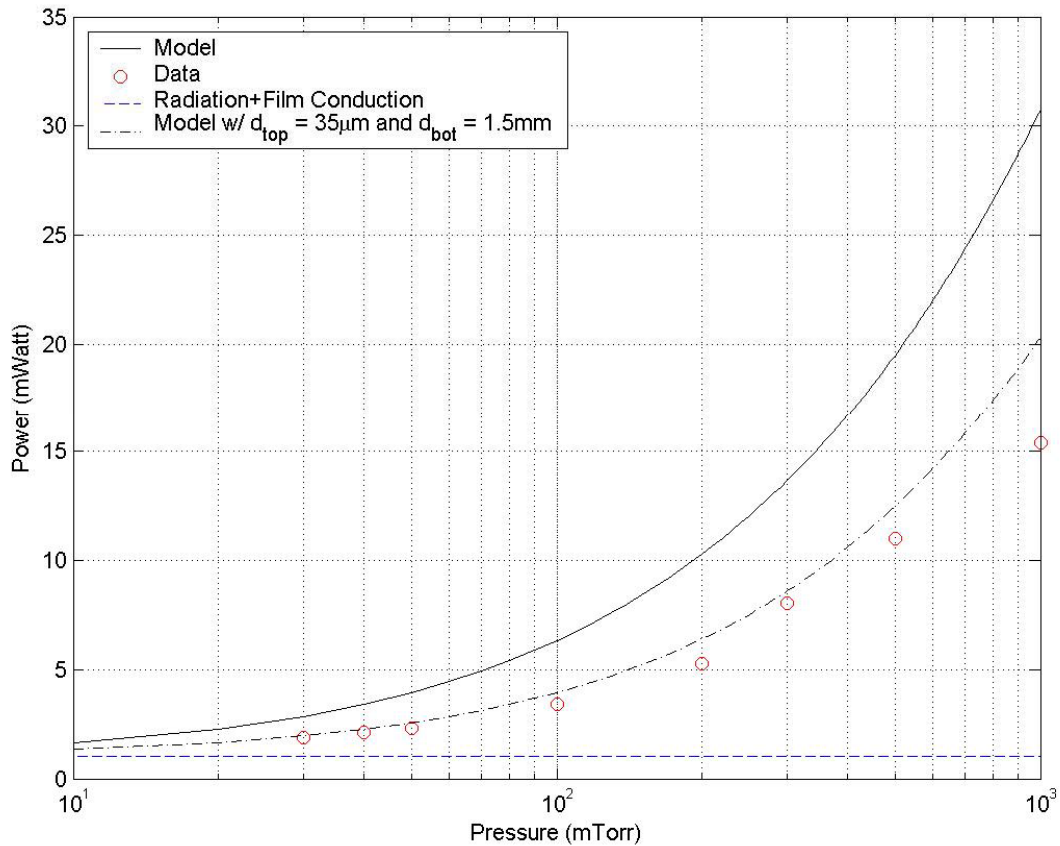


Figure 2 – Model with Experimental Data

Discussion

Several crude assumptions were made in developing the model. The values for the effective cross sectional areas used in the calculation, and the assumption of a constant temperature distribution across the resistor are gross oversimplifications. It is also assumed that the bulk silicon package remains at room temperature, and that there are no thermal boundary resistances in the system. Introducing thermal boundary resistances will present finite temperature differences at the various interfaces, invalidating the assumptions made about the temperature distribution. Utilizing perfectly diffusive boundaries and perfectly planar surfaces makes modeling the system easier but introduces many inaccuracies.

Looking at the experimental data in Figure 2, we see that at low pressures, the power dissipated in the test structure approaches the dashed line. This line corresponds to the heat transport of conduction across the membrane and of radiation. Since the heat conduction through gases should approach zero as the pressure approaches a pure vacuum, we would expect the data to be limited by the value indicated by the dashed line. Such a result indicates that the modeling of the two heat transport mechanisms represented by the dash line is quite accurate but we must keep in mind the assumptions used.

In the model, the pressure dependence of the heat conduction through gases correlates fairly well to the experimental data. We see

that the discrepancies are smaller at lower pressures and greater at higher pressures. A possible explanation is human error and the lack of instrumental precision at the higher pressures. A more reasonable explanation is that the assumptions used to arrive at Equation 6 were poor. The thermal conductivity of air is strongly dependent on the value used for d_{top} and d_{bot} . Since the packaged device does not comprise of infinite parallel plates, the effective distances should be greater than those used in the calculation. As we can see in Figure 2, increasing the values for d_{top} and d_{bot} significantly increase the correlation between model and experimental data.

Future Work

A model which is more rigorous can be developed in the future. One can include a finite element analysis of the resistive heater and membrane combined to obtain a more accurate temperature profile. Having a more precise temperature at points on the membrane will provide a significant boost in the potential of the model. The inclusion of partially diffusive boundaries and thermal boundary resistance can possibly increase the accuracy of the model. Factoring in the effects from the other surfaces not included in this model, planar and non-planar, is also an important consideration. Since classical effects are significantly in the conduction of gases, the actual geometry of the package and device needs to be considered thoroughly.

Once an accurate model is achieved, the understanding of the underlying heat transport mechanisms can be applied to developing a model for the fuel cell and thermophotovoltaic systems to be packaged. Having a reliable model before experimental data is collected will allow the researcher to foresee potential issues and optimize or changes their designs accordingly. This would be extremely beneficial since the

fabrication process can be lengthy and costly.

Summary

A second order model that incorporated classical size effects was developed to provide understanding and insight into experimental data. Data was collected from a microfabricated thermal conductivity pressure sensor which serves as a test device to evaluate a glass-frit vacuum packaging scheme. Good correlation is seen between the model and the data but the model is far from complete. Despite the lack of perfect convergence, the model provides information about the primary heat transport mechanisms in the packaged device. The developed model in this paper is a useful tool for researchers, and serves as a first step towards obtaining an ideal model.

References

- [1] Chou, J. 2002. A study of vacuum packaging methods for a microfabricated suspended tube reactor, M.Eng. Thesis, MIT
- [2] Chen, G. 2004. Nanoscale energy transport and conversion. p. 282-323
- [3] Chen, G., Borca-Tasciuc, D., Yang, R.G. 2004. Nano Heat Transfer. Encyclopedia of Nanoscience and Nanotechnology. Cambridge, USA. American Scientific Publishers 10 p. 1-30
- [4] Holmes, W., Gildemeister, J.M., Richards, P.L. 1998. Measurement of thermal transport in low stress nitride films. Appl. Phys. Lett. 72(18) p. 2250-2252
- [5] Zink, B.L., Hellman, F. 2004. Specific heat and thermal conductivity of low-stress amorphous Si-N membranes. Solid State Communications 129. p. 199-204